Australian Acoustical Society Conference,
Joondalup, Australia. 15-17 November 2000.

Acoustic Propagation Prediction in Shallow Water

Justin P. Hoffman[1], John D. Penrose[1], and Darryl R. McMahon[2]

[1]Curtin University of Technology, [2]Defence Science and Technology Organisation, Australia.

Abstract

An acoustic propagation experiment was conducted on 17 May 2000 in a shallow water site off the Perth metropolitan coast with the view of obtaining reflection and refraction data to contribute to developing a geoacoustic model of the area. The site proposed has constant bathymetry, though the geological properties of the site are not well known. The experiment used two hydrophones, one situated mid-water and the other moored to the seabed to explore the possibility of receiving head waves. The acoustic sources used were a 20-cui air gun and imploding sources comprising 60W and 75W light globes and purpose built evacuated spheres.

From the air gun data head waves were observed and reduced arrival time vs. range data are discussed in this paper. The travel time data of the implosive sources were particularly useful, in conjunction with Differential Global Positioning System (DGPS) data recorded at 1 second intervals, for an accurate assessment of horizontal separation between the source and receiver due to their impulsive nature. This affords an accurate analysis of the head wave signals, given that the source and receiver depths are known accurately. The detection ranges of the implosive sources is investigated, where the comparatively weak light globe sources were detected to approximately 1.2 km. Head waves were not excited by the implosive sources.

Introduction

This paper describes acoustic propagation measurements using a 20-cui air gun and implosive sources in shallow water. The measurements were made on 17 May 2000 in shallow water off the Perth metropolitan coast. The positions of the tracks were specified so that the seabed depth would be relatively constant along their lengths. The seabed properties along these tracks were not well known. In addition to the acoustical data, oceanographic data was taken. Water-column temperature and salinity profiles were measured at two positions. Salinity measured by the CTD was however found to be unreliable. Figure 1 illustrates the experiment location.

Light bulbs in particular have been the topic of interest as an implosive underwater acoustic source by a number of authors recently (Heard *et al.* 1997, Chapman *et al.* 1997). Their advantages include ease of field use, a reduced primary pulse and bubble pulse duration that may be useful for shallow reflection work, and operation depth. However, their energy output is generally low and there is concern that these sources do not output sufficient energy for sub-bottom reflections to be distinguished from noise in the water column. Their potential usefulness in shallow reflection work may be reduced further by the fact that they can be very broadband sources, depending primarily upon internal gas pressure. This is particularly applicable to the evacuated spheres, where in a recent study by two of the authors (Hoffman & Penrose, 2000) it was found that there is significant energy even at frequencies as high as 5kHz. Consequently it is a concern that the energy at such high frequencies (1kHz and above) will be lost to an absorptive seabed. The results of the propagation measurements performed using light bulbs and purpose-built evacuated spheres are discussed in this paper.

From analysing the recordings on both mid-water and bottom mounted hydrophones it was found that head waves were generated by the air gun. Given that the geological properties of the experiment site are not known well, the head waves offer a useful insight and are discussed in this paper. In the simple method of interpreting a refraction profile, the following assumptions were made:

1) The sound speed in the water column is independent of both depth and range,
2) The seabed sound speed is independent of range,
3) The seabed sound speed profile is a monotonically increasing sequence of uniform layers that are sufficiently thick for the interfaces to yield resolvable head waves at low frequencies,
4) Each interface in the seabed is flat and smooth,
5) The waveguide itself does not yield waveform spreading (through dispersion) that is sufficient to overlap the head wave arrivals.

To varying degrees, these assumptions are likely to be less applicable in shallow water than in deep water i.e. it is more difficult to find regions of horizontally uniform stratification. In any water depth, the first seabed layer

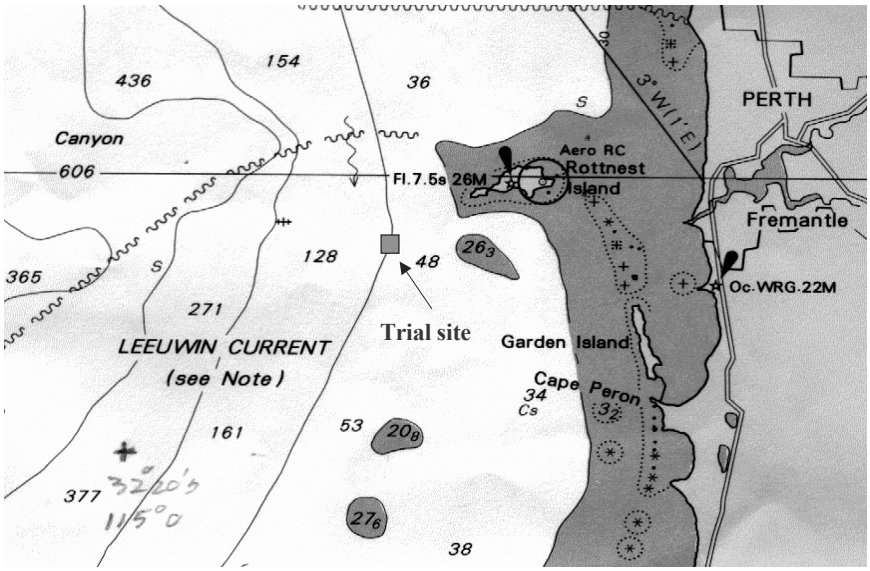

Figure 1: Experiment location where acoustic transmissions were measured. Depth contours are in metres.

usually consists of unconsolidated sediment and will therefore exhibit a significant and continuous increase in sound speed with depth. If a head wave from an unconsolidated layer were detected, then the question of how the sound speed profile below the interface affects the sound speed would need to be addressed. By close examination of the results, it should be possible to conclude whether the assumptions apply to a particular case. If for example a positive sound speed gradient exists, then in the time-distance plane a curvature of the arrival lines should be observed.

The main emphases of this paper are on presenting results and examining the quality of those results. For each head wave, results are presented for the compressional sound speed c_p and depth of the contributing interface in the seabed. These are determined from measurements of the reduced travel time of the head waves i.e. arrival time before the direct path (water borne) arrival.

Field Measurements

The acoustic receivers were Brüel and Kjaer 8104 and GEC Marconi SH101-X hydrophones, positioned at approximately 100m (on the seabed) and at 47m depth respectively. The sound sources were a 20-cui airgun positioned at approximately 8m depth when drifting and approximately 5m when towed, and implosive sources (light globes and evacuated spheres) imploded at approximately 40m depth. The light globes were 6cm in diameter and the evacuated spheres were 8cm in diameter.

The experiment can be broken up into 4 tracks. The first three were "drift" tracks, whereby the vessel was allowed to drift away from the moored recording package. Each drift track followed (roughly) the 100m depth contour in a southwesterly direction. During each of these drifts the air gun was fired at 10-second intervals. The implosive sources were lowered to 40m depth and imploded when the air gun was switched off. As soon as the implosion was complete, the air gun was switched back on to fire at 10-second intervals. Each drift was performed in this manner between 100m and 1000m range. After the conclusion of the third drift (approximately 1.2km range), the vessel steamed away at approximately 2.7 kts with the air gun in tow at approximately 5m depth. The air gun was fired at 30-second intervals. The vessel maintained a constant bathymetry track (along the 100m contour) until DAT recording time expired.

The horizontal range between the moored recording package and the shots were determined from the difference in DGPS positions of the shot and the DGPS position of the recording package. This was compared to the horizontal separation calculated from the arrival times of the various propagation paths in the evacuated sphere time series. The evacuated sphere records were used due to their short pulse duration, meaning the arrivals from direct, surface reflected, and multiply reflected paths are easily time separated. The ranges calculated from these two methods are within 1% of each other.

The bathymetry along each track was obtained using the ship's Furuno FCV-581 echo sounder, operated at 200 kHz throughout.

Geoacoustic Profile

Table 1 describes a geoacoustic profile of the experiment site, derived from personal communication and a PhD thesis by Collins (1983). Literature concerning the geological properties of the area is

Layer and thickness (m)	c_p (m/s)	c_s (m/s)	α_p (dB/λ)	α_s (dB/λ)	ρ (kg/m^3)
water column (102m)	1530	-	-	-	1025
medium sand (0.5m)	1600	-	0.5	-	1600
boundstone /soil (4m)	1700	-	0.5	-	1700
carbonate (~300m)	2500	1100	0.1	0.2	2100
unknown (basement)	3500	1500	0.1	0.2	2300

Table 1: Interpreted geoacoustic profile of the experiment site. Geoacoustic properties shown are based on data derived by Hamilton (1980).

sparse. It is expected that there are two thin layers of sediment at the surface of the seabed. The first layer is a thin veneer of medium-grained sand, typically less than 1m in thickness. Below this is a layer approximately 4m thick consisting of boundstone and soil. Below these layers is an unnamed carbonate formation, probably between 300 and 400m in thickness. At this stage it is not known what comprises the seabed below this layer. Compressional and shear sound velocities, attenuation coefficients, and associated densities have been interpreted from literature such as Hamilton (1980).

Data Analysis

Implosion Analysis

The purpose of the implosive sources was to investigate their properties and establish whether they are useful as underwater acoustic sources. The evacuated spheres, though extremely broadband due to their short pulse duration, are particularly useful in establishing multiple reflected paths.

The theoretical resonant frequency of an evacuated sphere or light globe implosion was approximated by Minnaert's resonant frequency equation,

$$f_0 = \frac{1}{2\pi R_0}\sqrt{\frac{3\gamma p_0}{\rho}}\,, \tag{1}$$

which describes the resonant frequency of a spherical gas bubble of radius R_0 in a liquid, undergoing low-amplitude simple harmonic motion. f_0 is the theoretical resonant frequency, R_0 is the mean bubble radius, p_0 is the hydrostatic pressure, ρ is the density of the surrounding fluid, and γ is the ratio of specific heats for the gas within the bubble. This expression assumes that heat exchanges and surface tension effects are negligible.

The source level of the light globes and evacuated spheres at range is simply

$$\text{SL} = 20 \log (\text{Peak Pressure}) + 20 \log (r) \tag{2}$$

where r is the direct distance between source and receiver.

Head Wave Analysis

Each of the air gun recordings at ranges between 400m and 5.5km contained precursors to the water borne arrival which have been interpreted as refraction arrivals that travelled along the seabed or sub-bottom interfaces. Only the signals received by the hydrophone positioned on the seabed are examined in this paper.

The stacked waveforms of shot arrivals on the final track were examined with the aim of identifying multiple series of pulses whose arrival times appeared to form a linear trend over range. The time of the onset of each signal was observed. From spectral analysis it was found that the head waves have a very narrow bandwidth, centred around 30 Hz, which is identical to the bubble pulse frequency of the air gun used.

The simplest method at hand to stack the waveforms was to align the direct water arrival of each signal and plot the result as reduced travel time with range. This means that to determine the velocity of the head wave (c_p), the actual arrival time, as determined by

$$t = r/c_p + t_0 \tag{3}$$

where r is the range and t_0 is the time axis intercept of the distance-time plot, needs to be rearranged in terms of the reduced travel time. Since the reduced travel time, here assigned the variable x_r, is only a shift in actual travel time by the direct path time (r/c_w), it may be written that

$$x_r + r/c_w = r/c_p + t_0 \tag{4}$$

which may be rewritten as

$$x_r = t_0 - r(1/c_w - 1/c_p) \tag{5}$$

where c_w is the speed of sound in the water column. Thus it is a simple matter of rearrangement to determine the head wave velocity:

$$1/c_p = 1/c_w - 1/v \tag{6}$$

where v is the gradient of the distance-reduced travel time graph.

The depth of the shallowest interface was obtained by first assuming that it coincided with the seabed. The depth was obtained from the time intercept t_0 in equation (5).

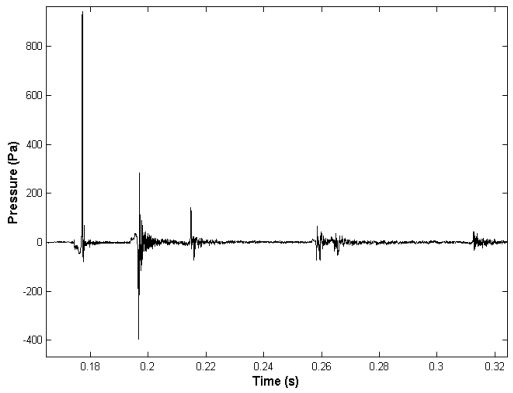

Figure 2: Time series of an evacuated sphere implosion at 137m range, illustrating the time separation of the various in-water arrivals. The sphere was imploded at 40m, where the receiver was positioned at 47m depth.

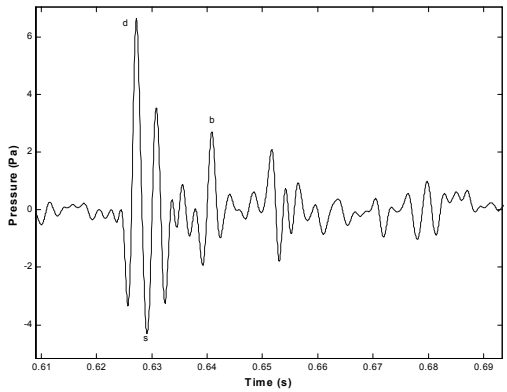

Figure 3: Light globe implosion, filtered through the band 10 to 500 Hz, at 1.2km range. Propagation path arrivals distinguished are **d** – direct path, **s** – surface reflection, and possibly **b** – bottom reflection.

Results

The Water Column

Two CTD casts were taken during the acoustic transmission measurements. From the results obtained the water column was virtually isospeed to the seabed, with an average value of 1530 m/s.

In the head wave interpretation the depth-dependence of the water column sound speed was taken into account by using the average value.

Implosive Sources

Figure 2 illustrates the time series for the shortest-range evacuated sphere implosion made (137m). Multiple reflection paths originating within the water column are easily observed. Given that the thin layers depicted in Table 1 may exist, a shallow sub-bottom reflection should appear very shortly after the bottom reflected arrival at t = 0.215s. The signal should be positive in magnitude since it would be a reflection from a positive reflection coefficient interface. However it does not look likely at this stage that such a reflection could be resolved. There exists a negative magnitude spike shortly after the arrival of the bottom reflection, though this is mostly likely to be an artefact of the original signal's small bubble pulse.

Source	Depth (m)	Average Source Level (dB re 1μPa @ 1m)
Light globe	40	205.4
Evacuated Sphere	40	222.3
Air gun	8	218.7

Table 2: Comparison between average peak source level of 36 light globe, 7 evacuated sphere, and 444 air gun transmissions. Source levels are referred to a distance of 1m.

The fact that a sub-bottom reflection is not immediately obvious may not be completely due to the broadband nature of the source but rather due to a low impedance/velocity contrast between any shallow sub-bottom layers. Indeed, since the first "layer" of medium grained sand is only 0.5m in thickness, the bottom reflection received at t = 0.215s may in fact be from the boundstone/soil layer. It remains to be seen however if techniques such as *deconvolution* may be useful to extract the Earth's impulse response from the received signal to infer any sub-bottom reflection occurrences.

Figure 3 illustrates the received signal from a light globe implosion at 1.2km range, filtered through the band 10 to 500 Hz to remove the low frequency flow noise at the midwater receiver and other high frequency components. The reception range was suprising, considering the comparatively low output energy of these sources. However, the inter-water column reflections are not easily observed in this record. This, though attributable to the low output energy of the source, is also attributable to the fact that the pulse duration and the experimental geometry do not allow time separability of the arrivals.

Table 2 compares the average of the peak source levels of 36 light globe, 7 evacuated sphere, and 444 air gun transmissions, carried out between 100m and 1.2km range, referred to a distance of 1m. The difference in peak source level between the light globes and evacuated spheres is attributable primarily to the difference in internal gas pressure. To a lesser degree, the difference in size (radius) will be a contributing factor in this case. It is interesting to note that the peak source level of the evacuated spheres is higher than that of the air gun, albeit at 40m depth compared to the air gun's depth of 8m.

Refraction Profiling Data

The signal stacks for the final track of the experiment are shown in Figure 4 [(a) for range up to 2km, (b) for range to 5.5 km]. As mentioned previously, the easiest way to make the precursors readable on a stacked display was to stack the signals such that each were aligned by the water-borne arrival. In order to present a constant amplitude for each signal, the signals have been normalised to the same peak-to-peak amplitude. For each stack plot, diagonal lines were fitted visually to the onset of the head waves. There are two head waves marked in this fashion. One is from a shallow interface (close to the water/seabed interface) and is marked by a dashed line in Figure 4(a). The other is from a deeper interface and is marked by a solid diagonal line, also in Figure 4(a). Figure 4(b) illustrates shots between 2km and maximum range, approximately 5.5km. Unfortunately, after approximately 4km the distinction between head wave arrival and noise becomes increasingly difficult and no definite trend can be established.

Features of the Waveforms

The waveforms presented in Figure 4(a) and (b) exhibit the following properties:

- the precursors have significantly narrower bandwidth than the water waves,
- the phases of the initial peaks of the precursors are randomly positive or negative.

The finding that most precursors are narrow band (with a peak near 30 Hz) is consistent with their classification as head waves rather than modal ground waves.

A good example of the variation in phase of the initial peak of the head waves was obtained on the last track from shots at ranges of 2.28 and 3.06 km and is illustrated in Figure 5. It can be seen that the phase of the closest shot is negative and changes to positive between the third farthest and the farthest shot illustrated (the second farthest shot still contains a small negative precursor). To describe this phase change mathematically, the distance over which this phase change occurs can be related to the wavelength of the head wave. The head wave velocity illustrated in Figure 5 was found to be 2925 m/s, so it's wavelength at 30 Hz would be approximately 97m. If the change in phase was taken to occur between the second farthest and the farthest shot i.e. a shot separation of 145m, then the change in phase over 145m would be 1.5 cycles or approaching –90°. There will always be some error in reading the travel time of a head wave, so it was decided that less error would be made by reading the first peak, regardless of phase, rather than reading the first peak of a particular phase.

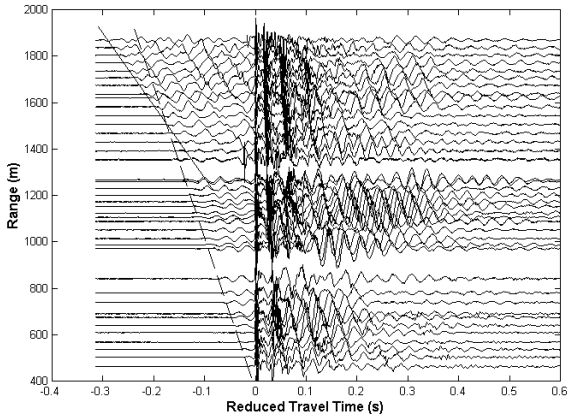

(a)

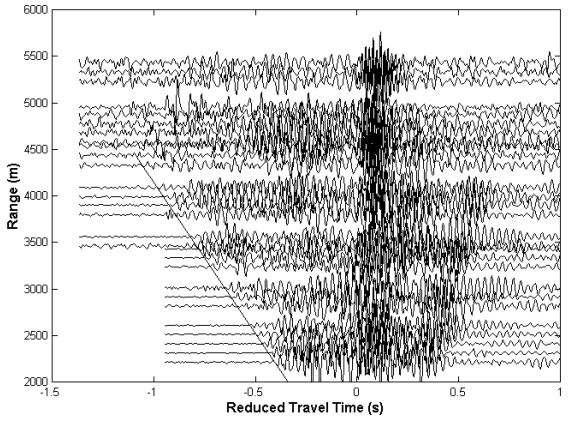

(b)

Figure 4: Signals from the final track stacked onto the range-reduced travel time plane. (a) Range to 2km, entire signal, (b) range to 5.5km, entire waveform (filtered through the band 14 to 70 Hz). Key to diagonal lines: ----- expected arrival of the shallow layer head wave, — expected arrival of the deep layer head wave. The solid line in (b) indicates the same head wave as the solid line in (a).

Interpretation of the Data

Simple interpretation of the data has yielded two head wave structures, as illustrated by the diagonal lines drawn on Figures 4(a) and (b). The first head wave arrival (steepest gradient) has however originated from below the water/seabed interface. The sound speed derived for this layer is 1930 m/s. According to Hamilton (1980), sound speeds up to 2000 m/s indicate that the sediment is of a calcareous nature (carbonate). From our knowledge of the region, this means the sediment is probably moderately cemented calcarenite. Since this was the first detected layer, an analysis concerning it's depth in relation to the water column depth was conducted and revealed that it exists approximately 3m below the water/seabed interface. Why a head wave was not excited from the surficial sediments is not known, though it is most probably due

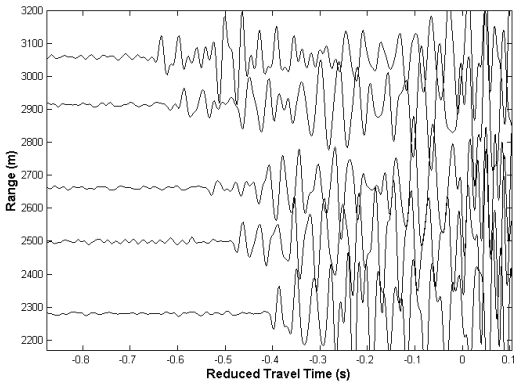

Figure 5: Detailed head wave precursors of five shots filtered through the band 14 to 70 Hz, illustrating the change in phase of the initial peak.

Layer and thickness (m)	c_p (m/s)	c_s (m/s)	α_p (dB/λ)	α_s (dB/λ)	ρ (kg/m^3)
medium sand (0.5m)	1600	-	0.5	-	1600
boundstone (4m)	1700	-	0.5	-	1700
calcarenite (327m)	1930	550	0.2	0.4	2000
chalk (basement)	2925	1300	0.1	0.2	2300

Table 3: Revised geoacoustic profile of the experiment site off Perth metropolitan coast.

to the fact that these layers are too thin to yield head waves.

The depth of the next interface below the seabed was then computed using the geometry of refraction paths for a simple two (horizontal) sediment layer problem and found to be 330m. The compressional sound speed of this interface, as indicated by the solid diagonal line in Figures 4(a) and (b), was found to be 2925 m/s. From Hamilton (1980) it would appear that this layer is similar to chalk, a consolidated and cemented sediment.

A modified geoacoustic profile of the region is considered in Table 3 for comparison with the initial estimate depicted in Table 1. The shear velocities, compressional and shear attenuation coefficients, and densities for these layers have been interpreted from Hamilton (1980).

Conclusion

Imploding acoustic sources offer potential advantages in terms of operation depth, ease of field operation, bandwidth for shallow reflection purposes, and a significantly reduced bubble pulse presence. Whilst their *peak* energy output may be relatively high, as shown in Table 2, their overall energy output is generally low. However, the ability to detect a light globe implosion at 1.2km range is promising.

Using a sound source such as an air gun and a hydrophone on the seabed it is possible to measure head waves from interfaces that are close to (indistinguishable from) the seabed. Their velocities may be determined from their arrival times in the range-time plane. Of the only track studied here, one such head wave was found and its velocity was calculated to be 1930 m/s. Head waves from deeper interfaces can also be measured using this technique. From this experiment a layer was found at 330m beneath the water/seabed interface, where its velocity was calculated to be 2925 m/s.

The amount of data obtained for the seabed may be limited by incoherence of the signals, especially 4km onwards. Spacing between shots was not a problem since, on average, the shot spacing was approximately 140 m between 1.2 km and 5.5 km range. Curvature in the range-reduced travel time plots was not observed, so it may be concluded that there is no evidence of sub-bottom sound speed gradients.

Acknowledgment

The authors acknowledge the valuable assistance provided by Mr Robert McCauley and Mr Malcolm Perry from the Centre for Marine Science and Technology (Curtin University) in preparing for and carrying out the experimental work reported here. We also thank Mr Ahmad Zakaria (Curtin University), Mr Damien Killeen (Defence Science and Technology Organisation), and Mr Alessandro Ghiotto (Nautronix) for their valued assistance during the experimental work.

References

[1]. Heard, G. J., McDonald, M., Chapman, N. R., and Jaschke, L., (1997), "Underwater light bulb implosions: A useful acoustic source", *Oceans 97*, *M.T.S./I.E.E.E. Conference Proceedings*, vol. 2, (2), pp. 755—762.

[2]. Chapman, N. R., Jaschke, L., McDonald, M. A., Schmidt, H., and Johnson, M., (1997), "Matched field geoacoustic tomography experiments using light bulb sound sources in the Haro Strait Sea trial", *Oceans* 97, *M.T.S.*/I.*E.E.E. Conference Proceedings*, vol. 2, (2), pp. 763—768.

[3]. Hoffman, J. P., and Penrose, J. D., (2000), "Long range acoustic propagation prediction in shallow water", CMST Project 182, Report no. C00-10, Curtin University of Technology.

[4]. Hamilton, E. L., (1980), “Geoacoustic modeling of the sea floor”, *J. Acoust. Soc. Am.*, 68, **5**, pp. 1313—1340.